Approximate Distance Fields with Non-Vanishing Gradients

Arpan Biswas, Vadim Shapiro *

Spatial Automation Laboratory
University of Wisconsin-Madison [1]

Abstract

For a given set of points S, a Euclidean *distance field* is defined by associating with every point p of Euclidean space E^d a value that is equal to the Euclidean distance from p to S. Such distance fields have numerous computational applications, but are expensive to compute and may not be sufficiently smooth for some applications. Instead, popular implicit modeling techniques rely on various approximate fields constructed in a piecewise manner. All such constructions lead to sacrifices in distance properties that have not been properly studied or characterized.

We show that the quality of an approximate distance field may be characterized locally near the boundary by its order of normalization and can be studied in terms of the field derivatives. The approach allows systematic quantitative assessment and comparison of various construction methods. In particular, we provide detailed analysis of several popular field construction methods that rely on set decompositions and *R-functions,* as well as identify the key factors affecting the quality of the constructed fields.

Key words: Distance functions, distance fields, approximate distance functions, gradients, curves, surfaces, R-functions

* Corresponding author.
Email addresses: arpan@sal-cnc.me.wisc.edu (Arpan Biswas), vshapiro@engr.wisc.edu (Vadim Shapiro).
[1] Complete address: 1513 University Avenue, Madison, WI 53706

1 Introduction

1.1 Motivation

Given a point set S, the Euclidean distance field is a mapping $f : E^d \rightarrow R$ that associates with the every point of space a value equal to the shortest distance to S. For brevity, we will refer to f as the distance field (or distance function) for S. Distance functions are unique, intuitive, and are well understood mathematically. Distance fields have numerous applications in modeling, planning, vision, image processing, visualization, and computer graphics (for example, see [1]). Without trying to be comprehensive, we will only mention some recent promising applications of distance fields. In layered manufacturing of solids with varying material composition distance fields are used to specify the properties of the material [2–5]. In engineering analysis, distance functions of boundaries of the domain are employed to introduce boundary conditions [6]. Distance fields allow straightforward construction of offsets [7,8] and to induce parameterization of curves and surfaces [9]. Level set methods for solving evolving interface problems depend on distance fields for initialization and assignment of extension velocities at points away from the evolving boundary [10]. In biomedical applications, the distance field is employed to construct n-dimensional models from sequences of $(n-1)$-dimensional cross-sections [11]. In computer aided geometric design and graphics, application of distance functions can be found for representing and modeling geometries [12–15]. In graphics, distance functions are employed for volume rendering [16] and for shape morphing [17,18]. Distance fields are also widely used in robot motion planning problems [19–21].

When a set S is represented using n geometric primitives, it is reasonable to expect that the distance from a point p to S should be computable in $O(n)$ time, or better if S is represented by using some hierarchical structure [12]. But unfortunately, computing the distance from p to a single geometric primitive (typically a curve or surface) usually requires a numerical iterative procedure [22,7]. Furthermore, the exact distance field is not sufficiently smooth for many engineering applications because the distance function is not differentiable at points that are equidistant from several points of S [23,24,5,18,19]. But differential properties are critical in many applications. Smoothness is also lost when a distance function to S is replaced by a piecewise linear approximation constructed as a minimum of distances to individual linear sections [25,26].

In order to achieve the desired smoothness, the minimum distance function is often replaced by various smooth approximations, such as Ricci function [27], blending functions [28], R-functions [29], convolution [30] and others. From these, Ricci and blending functions introduce additional errors into distance at the boundary of set S, while R-functions and convolution methods do not. Properties of the distance field near S are critical in many applications mentioned above. Consider the example in Figure 1. The approximate smooth distance fields for two line segments are shown in Figures 1(a) and (b) respectively. Figure 1(c) shows the field for the union of the two line segments constructed as a join of the two individual fields. [2] While the zero set of this field

[2] This particular join is described in detail in section 2.2 and relies on R-functions.

coincides exactly with the union of the line segments, a substantial distortion of the field is visible near the *joining point*, i.e. the point where the two segments are joined together. This phenomenon is known popularly as "bulging" and is a property of many joining methods.

(a) (b) (c)

Fig. 1. (a) and (b) are approximate distance fields of two line segments; (c) a combined field for the union of the two line segments constructed with the R-equivalence operation of order 2.

Ideally, we would like to use both R-functions and convolution techniques without introducing bulging. In fact, it is widely believed that convolution visibly eliminates bulging [30]. As we will explain below, unfortunately this is achieved at the cost of sacrificing important differential properties in the constructed distance field. Hence, this paper focuses mainly on R-function methods for constructing distance fields. In particular, one of the principal objectives of this paper will be to characterize the bulging effect by studying differential properties of distance fields near the joining points. The key concept is that of normalized approximation of a distance field introduced by Rvachev [31].

1.2 Normalized Approximation

A smooth approximation of the distance fields near the point set S can be characterized with the concept of normalization in the following sense. Suppose point p is a *regular* point on the boundary of set S, i.e., a point where a unit normal direction ν is well defined. By definition, the exact distance function f is 0 at p; the first partial derivative of f at p in the direction ν is equal 1 and *all* higher derivatives vanish. This corresponds to the intuitive fact that the value of f at a point that is distance δ away from p is equal to δ. A suitable m-th order approximation of f is a function ω that is obtained by requiring only *some* of the higher order derivatives to vanish, that is for all regular points p on the boundary of S:

$$\frac{\partial \omega}{\partial \bar{\nu}} = 1; \frac{\partial^k \omega}{\partial \bar{\nu^k}} = 0; k = 2, 3...., m \tag{1}$$

Such a function ω is called *normalized*[3] to the m-th order. Normalized functions behave like a distance function near its zero set (corresponding to the boundary of set S) and tend to smoothly approximate the distance function away from S. The loss of normalization is accompanied by local changes in field derivatives. Any decrease in gradient magnitude implies a slower growth of the field in some direction which visibly manifests itself as " bulging." Functions in Figure 2(b), (c), (d), (e), and (f) are approximate distance functions of a 'W' shaped B-spline curve of order 4, normalized up to the order 2, 3,5, 7, and 12 respectively. It is apparent, that with increase in the order of normalization the approximate distance functions behave more like the exact distance function, with substantially reduced bulging. However, normalization is a local property and does not guarantee that the function behaves as the distance function away from the boundary points.

Normalized functions are adequate substitutes for distance functions in numerous applications, including level set methods, meshfree analysis, material modeling and solution of geometric problems. For example, in the level set method, a function normalized to the first order is sufficient for assigning the extension velocity[10]. In meshfree analysis [6,23] and material modeling [5] functions normalized to a specified order are employed to model the rates of change of the function at the boundary. Algorithms proposed in [7,9] to construct offsets of curves and surfaces and also to parameterize them require normalized functions, and polygonization of an implicitly defined surfaces relies on iterative algorithms that converge faster when the defining functions are normalized[32].

There are two basic approaches to construction of normalized functions. It should be intuitively clear that *any* function with non-vanishing gradient may be scaled to behave as a normalized function. Appendix A shows the general procedure for normalization to the desired order, following [31]. However, constructing a smooth function with non-vanishing gradient is not trivial. For example, many fields defined by convolution methods are flat at the boundary, with precise behavior depending on the type of the selected kernel. Other difficulties with more promising kernels are briefly discussed in section 4.1.

The remaining alternative is to construct normalized approximations in a piecewise manner, and this is the approach studied in the remainder of this paper. The fields shown in Figures 1 and 2 are are fully normalized on all regular points of the boundary, but the normalization conditions are clearly violated at the corners and joining points, where the notion of normal is not even defined.

1.3 Scope and Outline

We propose a general method for constructing approximate distance fields for arbitrary trimmed curves and surfaces that combines the strengths of several known techniques. The basic idea is straightforward: we partition a given curve or surface into a union of segments, construct normalized functions for each segment, and then combine the individual normalized functions into a single

[3] This terminology is consistent with the term *normal* function that is often used synonymously with the distance function.

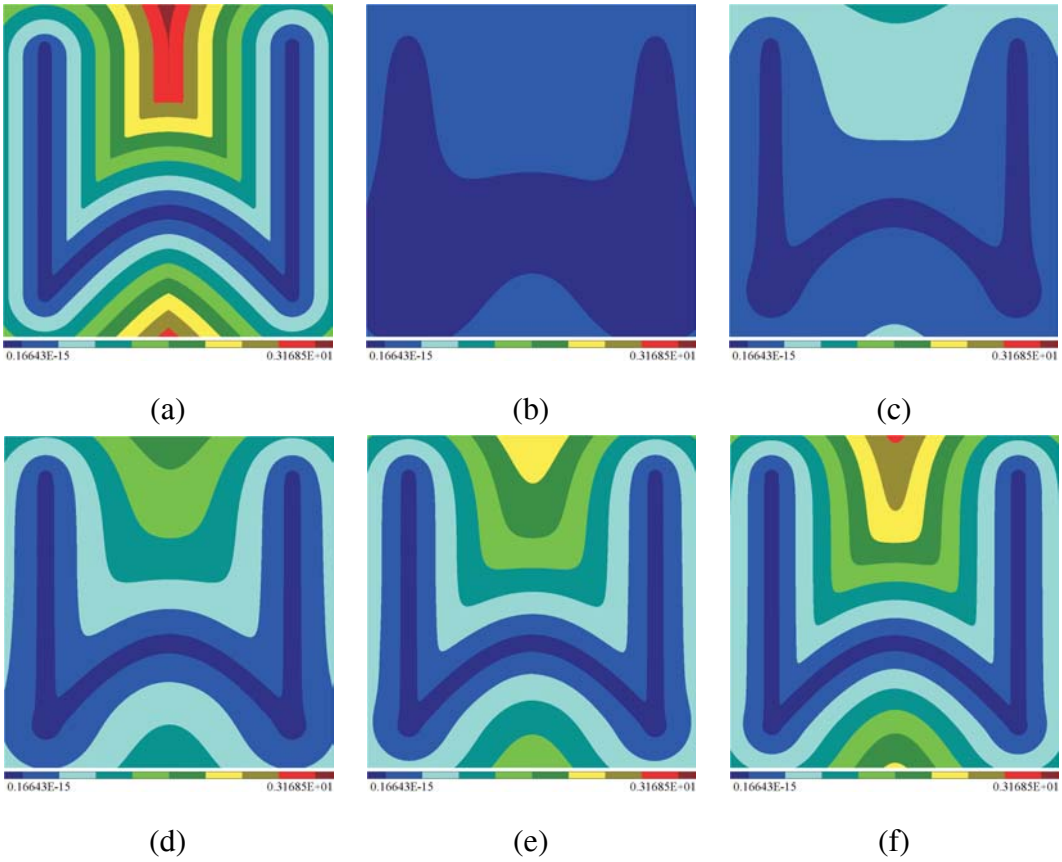

Fig. 2. Isolines of distance fields constructed from a 'W' shaped B-spline curve of order 4: (a) true Euclidean distance field; (b), (c), (d), (e), and (f) are smooth approximations of the distance function and these are normalized to the order 2, 3, 5, 7 and 12 respectively.

approximate distance field. The normalized functions can be constructed and combined using the techniques based on R-functions, as described in [29,31]. If the decomposition into segments is exact, then the zero set of the constructed field will coincide exactly with the original curve or surface. If the union of the segments approximates the original curve or surface, then so will the zero set of the constructed field. In this paper we study the approach based specifically on polygonization of curves and surfaces, but many of our observations also apply to other types of decompositions. We will assume that a given curve or surface is polygonized by any known technique. Then the normalized functions for each of the segments in the polygonization are constructed by trimming the carrier plane or line with a suitable *trim volume*. Finally, a single approximate distance field is obtained using joining operations on the individual normalized functions. The quality of approximation in the constructed functions is determined by two separate factors:

(1) the value of the field may not be zero at the original curve or surface but its magnitude is directly related to the error in the polygonization;
(2) the constructed field may not be normalized at all/some regular points of the original curve or surface where adjacent segments are joined.

In what follows, we study the quality of the constructed approximations for curves and surfaces in terms of their normalization properties. We provide specific bounds on the magnitude of the gradient near joining points, and identify intrinsic limitations of the proposed approach as well as promising directions for improving the quality of normalization.

The rest of the paper is organized as follows. Section 2 details the construction procedure and analyzes the properties of the constructed field for planar curves. Sections 3 builds on these observations and generalizes the method for curves and surfaces in E^3. Concluding section 4 summarizes our observations, briefly discusses alternative approaches and suggests several directions for further investigations.

2 Approximate Fields for Planar Curves

We will assume that a given planar curve can be polygonized to some precision ϵ measuring maximum deviation from the original curve. Many elegant algorithms for finding constrained polygonal approximation for most types of curves are available. For example, practical algorithms for finding the polygonal approximation of B-spline and Bezier curves are described in [33,34]. Thus, we focus on the two remaining steps of field construction: constructing normalized functions for individual line segments using trimming operations (section 2.1) and combining them into a single field using joining operations (section 2.2). Section 2.3 examines the quality of the constructed approximate field, and section 2.4 presents substantial experimental data supporting our analysis.

2.1 Trimming

The discussion in this section is a straightforward application of the trimming procedures described and studied in [29,35,36] for arbitrary implicitly defined curves and surfaces. Here, the same procedures are used to construct a normalized function for a straight line segment.

A line segment can be represented as the intersection of an infinite line and some trim region, e.g. a circular disk, as shown in Figure 3(a). A trimming operation produces a normalized function for the line segment, given normalized functions for the unbounded line and the trim region. In our case, the normal (signed distance) function $f(x, y)$ for a line passing through the end points (x_1, y_1) and (x_2, y_2) of the line segment is

$$f = \frac{(x - x_1)(y_2 - y_1) - (y - y_1)(x_2 - x_1)}{\sqrt{(x_2 - x_1)^2 + (y_2 - y_1)^2}} \tag{2}$$

The trim region is a disk of diameter $d = \sqrt{(x_1 - x_2)^2 + (y_1 - y_2)^2}$, with the center located at

$x_c = (x_1 + x_2)/2$, $y_c = (y_1 + y_2)/2$, and can be represented by an inequality $t(x, y) \geq 0$, where

$$t = \frac{1}{d}\left[\left(\frac{d}{2}\right)^2 - (x - x_c)^2 - (y - y_c)^2\right] \tag{3}$$

The factor $1/d$ scales the function t so that it is normalized to the first order.

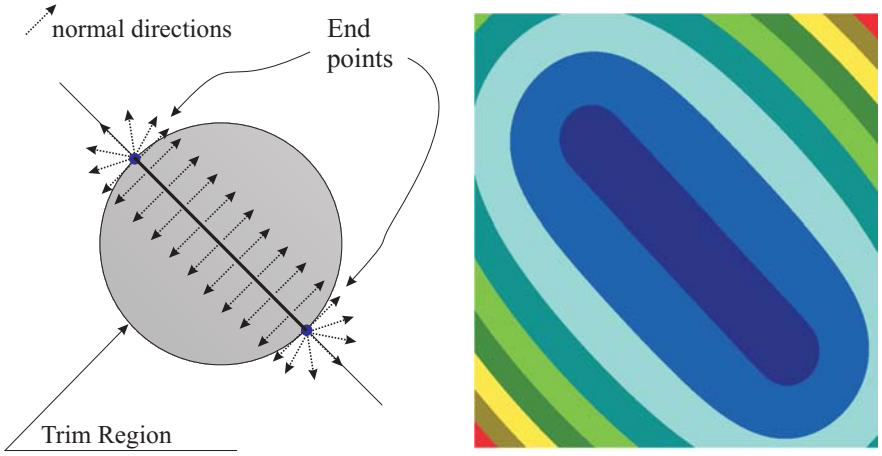

(a) (b)

Fig. 3. (a) Normalized function for a line segment is constructed by intersecting the unbounded line with a circular trim region. (b) Isolines of the constructed field.

A normalized function for the line segment, formed by intersection of the line with the circular trim region, may be constructed by several methods originally proposed by Rvachev [31] and analyzed in [29]. For example, the composite function

$$h = \sqrt{f^2 + \frac{(|t| - t)^2}{4}} \tag{4}$$

is zero exactly on the points of the line segment, positive everywhere else, and is normalized at all regular points of the segment. Strictly speaking, function h is not differentiable at its zero set, but its derivatives in the direction ν normal to the line segment are well defined. It is also easy to show that h is fully normalized at the regular points of the line segment. The differential properties of the constructed function h at points where h is not zero are determined by the differential properties of the functions f, t, and the trimming operation (4). Function h is continuous at all such points, except the points where $t = 0$, where h has second derivative discontinuity. If higher order derivative continuity is required, the trimming operation (4) may be generalized. For example, a slightly modified function

$$h = \sqrt{f^2 + \frac{(\sqrt{(t)^2 + f^4} - t)^2}{4}} \tag{5}$$

is twice differentiable at all points away from the line segment, including those where $t = 0$. This expression is basically the same as in (4), with term $|t|$ replaced by $\sqrt{(t)^2 + f^4}$. Geometrically, this could be also viewed as a global deformation of the trim region, and we will take advantage

of this technique for construction of smooth three-dimensional fields in section 3.2. Higher order continuity of t may be assured using analogous techniques [31].

Rvachev [31] proposed that the notion of normalization may be extended to situations where the normal direction may not be unique. This is accomplished by *redefining* the normal direction $\overline{\nu}$ at point $x \in S$, to be a direction in which there exists a point $p \notin S$ such that p is closer to x than to any other points of S [31,29]. This definition is consistent with the fact that the gradient vector of a distance function points in the normal direction in the neighborhood of all boundary points. Figure 3(a) shows normal directions of a line segment around its end point. With this new definition of normal, the constructed functions for the line segment are in fact normalized at *all* points of the line segment, including its end points (see Figure 3). Other methods for normalization and trimming operation for general curves and surfaces are described in [29].

To summarize, given normalized functions for an unbounded curve and a trim region, the trimming operations are capable of producing sufficiently smooth normalized functions for the trimmed segment. Given such functions for a number of segments representing or approximating a given curve, they may be combined into a single field using one of the *joining* operations described below.

2.2 Joining Operations

Joining two or more approximate distance fields h_i of line segments l_i can be considered a logical operation on the individual fields. We seek a single combined field $u(x, y) = F(h_1, h_2, \ldots, h_n)$ such that $u = 0$ on all segments and u is normalized to some order on all regular points of the segments. In other words, we need to replace the logical joining operation with an appropriate arithmetic operation F. This can be achieved by choosing F from one of many possible R-functions, as we now explain.

R-functions are real valued functions whose signs are completely determined by the signs of their arguments[35,31]. In other words, these functions work as Boolean switching functions. Every logical operation, such as negation($\neg$), conjunction($\wedge$), disjunction($\vee$) and equivalence($\sim$), correspond to infinitely many R-functions. For example, the arithmetic operation of multiplication xy corresponds to the logical operation of equivalence: it is only positive (true) when both x and y are positive (true) or negative (false). Therefore, the product is called an R-equivalence operation. But the product of R-equivalence with any positive function is also R-equivalence. Among many different possibilities [31], specific R-functions are chosen for their simplicity, differential, and computational properties. Henceforth we will use the symbols of the logical operation ($\wedge, \vee, \neg, \sim$) to denote their corresponding R-functions. The main result of the theory of R-function states that a logical predicate on a finite number of inequalities (of the same type) may be translated into a single inequality of the same type by syntactically replacing the logical operations with the corresponding R-functions. Equalities may also be combined by treating them as special types of inequalities. For additional details and references, the reader is referred to [35].

In the context of this paper, each segment l_i is represented by its normalized field h_i, with $h_i = 0$ on the points of the segment and positive everywhere else. At least two different types of R-functions may be used to perform the joining operation. These R-functions are R-conjunction ($\wedge$) and R-equivalence ($\sim$).

2.2.0.1 R**-equivalence** Consider two line segments l_1 and l_2 with their normalized fields h_1 and h_2. It should be clear that a distance field $u = F(h_1, h_2)$ for the union $l_1 \cup l_2$ should be zero whenever either h_1 or h_2 are zero, and positive anywhere both functions are positive. This naturally suggests an R-equivalence operation, for example setting $F(h_1, h_2) = h_1 h_2$. The only problem is that the resulting function is not normalized at the regular points of the original line segments. Fortunately, as we explain in section 2.3, another (scaled) R-equivalence

$$F(h_1, h_2) = h_1 \sim h_2 \equiv \frac{h_1 h_2}{\sqrt[p]{h_1^p + h_2^p}} = \frac{1}{\sqrt[p]{\frac{1}{h_1^p} + \frac{1}{h_2^p}}} \tag{6}$$

preserves the normalization of u to the order p on all regular points of the two line segments. Here p can be any positive integer. The rightmost expression for R-equivalence suggests that it can be viewed as the reciprocal of the p-norm of the vector $(\frac{1}{h_1}, \frac{1}{h_2})$. Note that as $p \to \infty$, $h_1 \sim h_2$ approaches $\min(h_1, h_2)$. This insight will prove useful in section 4.2. The field u in Figure 1(c) was constructed by joining h_1 and h_2 with the R-equivalence of order 2. Now if $h_1, \ldots, h_n$ are normalized functions for n line segments approximating a curve, then the function $u = h_1 \sim \ldots \sim h_n$ is an approximate distance field for the polygonization of the curve.

2.2.0.2 R**-conjunction** Another approach to joining takes advantage of the fact that the two line segments are represented implicitly by the inequalities $-h_1 \geq 0$ and $-h_2 \geq 0$. Then the union of the two line segments is defined by any R-disjunction operation as $-h_1 \vee -h_2$, or after applying De Morgan's law, by any R-conjunction as $h_1 \wedge h_2$. Amongst many different possibilities, the following is the simplest R-conjunction that preserves the normalization of its arguments through order $p - 1$ (see section 2.3).

$$F(h_1, h_2) = h_1 \wedge h_2 \equiv h_1 + h_2 - \sqrt[p]{h_1^p + h_2^p}, \tag{7}$$

where p can be any positive integer. For n segments, the joined approximate distance field is constructed as $u = h_1 \wedge h_2 \wedge h_3 \ldots \wedge h_n$.

In what follows, we examine the properties of the constructed fields in terms of their ability to approximate the normalized functions for the original curves. We shall see that the two joining operations are similar in terms of their normalization properties, even if they imply globally distinct approximate distance fields. We also note that the R-equivalence (6) operation is associative (which means that the constructed field does not depend on the order in which the individual segments are joined), while R-conjunction (7) is not [31].

2.3 Quality of Approximation

If the constructed function u were fully normalized and exactly zero on all points of the original curve, u would behave exactly as the distance function, at least in the neighborhood of the curve. But our construction process introduced two sources of errors mentioned earlier: approximation of the original curve and possible loss of normalization.

The effect of polygonization is that the constructed function u will not be zero on most points of the original curve S. Instead it will be zero on the set P of points on the segments in the polygonization. Now, consider a point q on the original curve S that lies in the neighborhood of P at a distance δ away, measured in the direction ν normal to P. The Taylor series expansion of the function u in the neighborhood of P in the direction ν yields:

$$u(q) = u\Big|_P + \delta \frac{\partial u}{\partial \nu}\Big|_P + \sum_{k=2}^{m} \delta^k \frac{\partial^k u}{\partial \nu^k}\Big|_P C_k + O(\delta^{m+1}) \tag{8}$$

The first term is zero. If u is normalized to the order m, then $\frac{\partial u}{\partial \nu} = 1$ in the second term and all the normal derivatives up to the order m in the third term are zero. It follows that

$$u(\mathbf{x}) = \delta + O(\delta^{m+1}) \tag{9}$$

We conclude that if a curve is approximated in such a way that the maximum deviation of the curve from the polygonal approximation is bounded by ϵ, then the maximum value of function u at the original curve is $O(\epsilon)$.

The above analysis assumes that the function u is normalized at all points of the polygonal approximation P. But, as we already observed in section 1, the joining operations preserve normalization on all regular points, but not in the neighborhoods of the joining points where bulging occurs. Consider what happens to the gradient of u in the neighborhood of a joining point when two segments with distance fields h_1 and h_2 are joined by any R-function $F(h_1, h_2)$. The partial derivatives of u are $\frac{\partial u}{\partial x} = \frac{\partial F}{\partial h_1}\frac{\partial h_1}{\partial x} + \frac{\partial F}{\partial h_2}\frac{\partial h_2}{\partial x}$ and $\frac{\partial u}{\partial y} = \frac{\partial F}{\partial h_1}\frac{\partial h_1}{\partial y} + \frac{\partial F}{\partial h_2}\frac{\partial h_2}{\partial y}$ and the magnitude of the gradient ∇u is determined by

$$|\nabla u|^2 = \left(\frac{\partial F}{\partial h_1}\frac{\partial h_1}{\partial x} + \frac{\partial F}{\partial h_2}\frac{\partial h_2}{\partial x}\right)^2 + \left(\frac{\partial F}{\partial h_1}\frac{\partial h_1}{\partial y} + \frac{\partial F}{\partial h_2}\frac{\partial h_2}{\partial y}\right)^2 \tag{10}$$

It is easy to check that for both R-equivalence (equation (6)) and R-conjunction (equation (7)), $\frac{\partial F}{\partial h_1} = 1$ but $\frac{\partial F}{\partial h_2} = 0$ when $h_1 = 0$, and $\frac{\partial F}{\partial h_2} = 1$ but $\frac{\partial F}{\partial h_1} = 0$ when $h_2 = 0$. Since h_1 and h_2 are normalized functions, the absolute value of their gradients near the corresponding line segments are 1. Therefore $(|\nabla u|)^2 = 1$ when either $h_1 = 0$ or $h_2 = 0$ (but not both). Similar types of calculations show that derivatives up to the order p vanish for R-equivalence and up to order $p-1$ for R-conjunction, when either $h_1 = 0$ or $h_2 = 0$. This confirms that R-conjunction preserves normalization through order $p-1$, and R-equivalence through order p on all interior points of the two line segments. However, normalization of u is not maintained near the joining points where

simultaneously $h_1 = 0$ and $h_2 = 0$. The magnitude of the gradient, ∇u, in the neighborhood of such points varies depending on the direction of approach [29]. Expanding equation (10), the magnitude of the gradient of the composite field may be written explicitly as a function of the individual gradients ∇h_1 and ∇h_2:

$$(|\nabla u|)^2 = \left(\frac{\partial F}{\partial h_1}\right)^2 + \left(\frac{\partial F}{\partial h_2}\right)^2 + 2\frac{\partial F}{\partial h_1}\frac{\partial F}{\partial h_2}\left(\frac{\partial h_1}{\partial x}\frac{\partial h_2}{\partial x} + \frac{\partial h_1}{\partial y}\frac{\partial h_2}{\partial y}\right) \tag{11}$$

$$= \left(\frac{\partial F}{\partial h_1}\right)^2 + \left(\frac{\partial F}{\partial h_2}\right)^2 + 2\frac{\partial F}{\partial h_1}\frac{\partial F}{\partial h_2}\left(\nabla h_1 \cdot \nabla h_2\right) \tag{12}$$

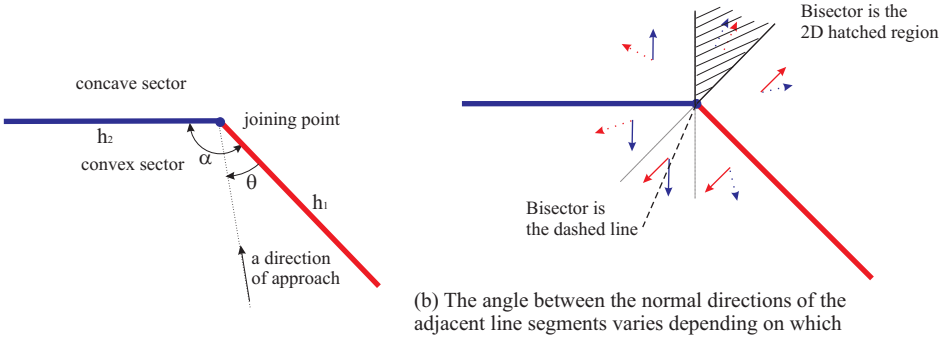

(a) The value of gradient in the neighborhood of the joining point depends on the angle between the line segments and the direction of approach.

(b) The angle between the normal directions of the adjacent line segments varies depending on which of the 6 sectors contains the direction of approach. Vectors show directions of gradients ∇h_1 and ∇h_2; solid vectors indicate that the direction of gradient does not change within the sector.

(a) (b)

Fig. 4. Normalization fails in the neighborhood of joining points

Because h_1 and h_2 are normalized in the generalized sense (i.e. in all directions) near the end points of the line segments, the term $\nabla h_1 \cdot \nabla h_2$ varies between -1 and +1, depending on the angle, α, between the line segments and the direction of approach, θ, to the joining point (see Figure 4). We can immediately conclude that the theoretical bounds on the magnitude of gradient ∇u are:

$$\left(\frac{\partial F}{\partial h_1} - \frac{\partial F}{\partial h_2}\right)^2 \leq |\nabla u|^2 \leq \left(\frac{\partial F}{\partial h_1} + \frac{\partial F}{\partial h_2}\right)^2 \tag{13}$$

To determine the precise bounds, one needs to examine the partial derivatives of the particular joining function F. Below we assume that F is R-equivalence; similar analysis applies when F is R-conjunction.

$$\frac{\partial F}{\partial h_1} = \frac{h_2^{p+1}}{(h_1^p + h_2^p)^{\frac{p+1}{p}}}; \qquad \frac{\partial F}{\partial h_2} = \frac{h_1^{p+1}}{(h_1^p + h_2^p)^{\frac{p+1}{p}}}$$

Changing to a polar coordinate system in the neighborhood of the point $h_1 = h_2 = 0$, these

equations become

$$\frac{\partial F}{\partial h_1} = \frac{\sin(\Phi)^{p+1}}{(\cos(\Phi)^p + \sin(\Phi)^p)^{\frac{p+1}{p}}}; \qquad \frac{\partial F}{\partial h_2} = \frac{\cos(\Phi)^{p+1}}{(\cos(\Phi)^p + \sin(\Phi)^p)^{\frac{p+1}{p}}}, \tag{14}$$

where angle Φ measures the direction in the (h_1, h_2) plane (see Figure 5(a)). Since h_1 and h_2 are non-negative functions, Φ varies between 0 and $\frac{\pi}{2}$ as the direction of approach, θ, in the Euclidean space varies from 0 to α (Figure 4(a)). It is not difficult to show that when $\Phi = \frac{\pi}{4}$, the term $(\frac{\partial F}{\partial h_1} + \frac{\partial F}{\partial h_2})$ reaches its minimum, and it never exceeds 1. Similarly, the term $(\frac{\partial F}{\partial h_1} - \frac{\partial F}{\partial h_2})$ never exceeds 1 and is identically 0 in the direction along $\Phi = \frac{\pi}{4}$. The precise relations between the magnitudes of the gradients and the direction Φ are determined by equations (14) and are plotted in figures 5(b), 5(c) and 5(d) for R-equivalence operations of order $p = 2$, 7, and 12 respectively. Observe, that for the gradient of u to be exactly equal to the lower bound 0, it is necessary that

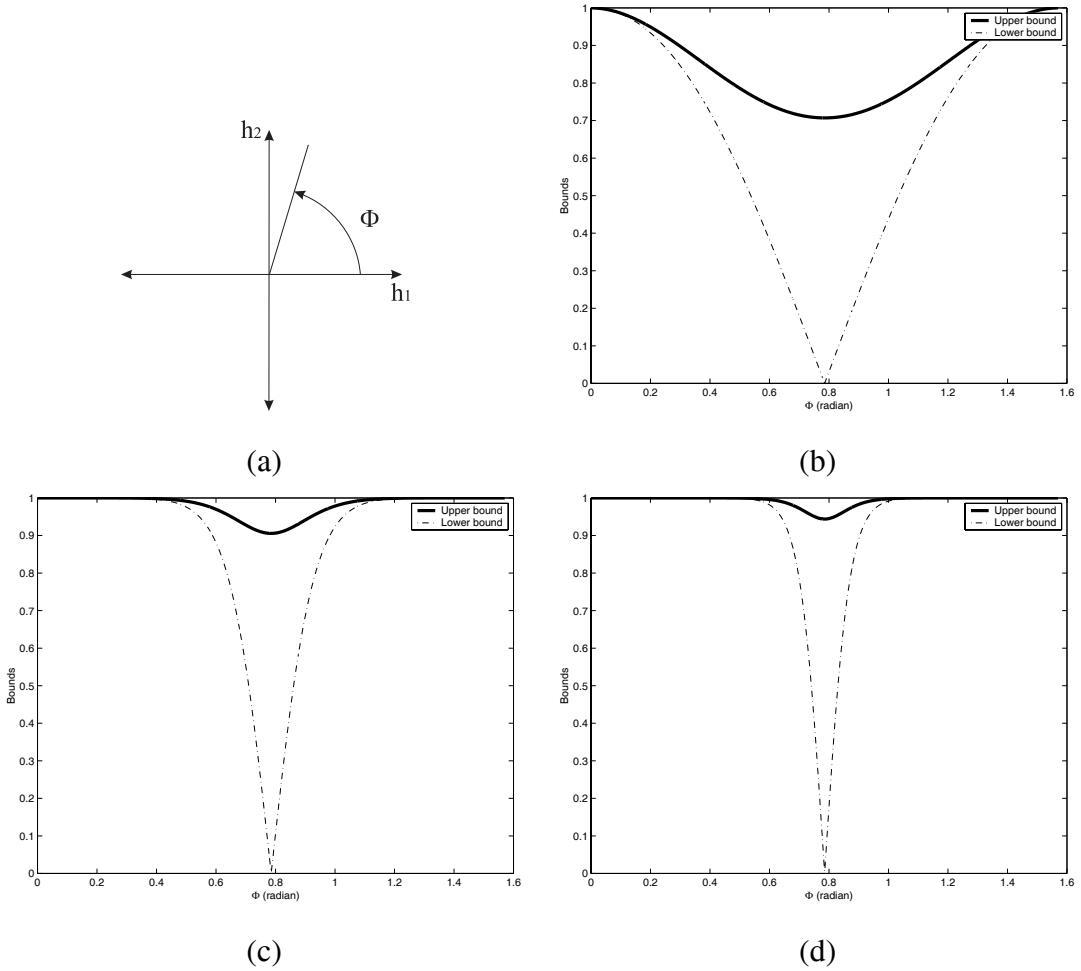

Fig. 5. Figure (a) shows coordinate system defined by the arguments of R-functions. Figure (b), (c) and (d) show the upper and lower bounds on the gradient of the R-equivalence operation of order p=2,7, and 12 respectively.

$\nabla h_1 \cdot \nabla h_2 = -1$. But this requires that some normal directions of the two line segments were

π apart, which is impossible for adjacent edges in a valid polygonization of a curve. Thus, we conclude that the magnitude of the gradient of the approximate distance field constructed with R-equivalence as a joining operation always lies strictly between 0 and 1 near the joining points. A similar procedure may be used to show that when R-conjunction is used as a joining operation, the magnitude of the gradient is also bounded strictly between 0 and 1 near the joining point.

The above analysis completely characterizes the bulging effects in the neighborhood of joining points. The minimum value of the gradient always occurs on the bisector between (i.e. set of points equidistant from) the two segments (Figure 4(b)). In the concave sector (where $\alpha > \pi$), this bisector is a two-dimensional region where the value of the gradient is constant but cannot exceed $(\frac{\partial F}{\partial h_1} + \frac{\partial F}{\partial h_2})$. It is also clear (both from the expressions and from the plots) that increasing the order of normalization, p, reduces the range of directions with low gradient values, and also brings the upper bounds closer to 1, but never reaches it. In the convex sector (where $\alpha < \pi$), the minimum value of the gradient occurs on the bisector of angle α and is a function of α: a smaller α leads to a lower gradient, but $|\nabla u|$ does not vanish anywhere in the neighborhood of the joining point.

Functions in Figure 6 were constructed by joining distance functions of two horizontal line segments of unit length. The two line segments intersect at a joining point. The three functions in Figure 6 (a), (b) and (c) were constructed with R-equivalence of order 2, 7 and 12 respectively. In all three of these functions, the bulging of isosurfaces near the joining point is visible. However, it is apparent that with increase in the order of the R-equivalence operation the bulging effect diminishes and this observation is supported by analysis.

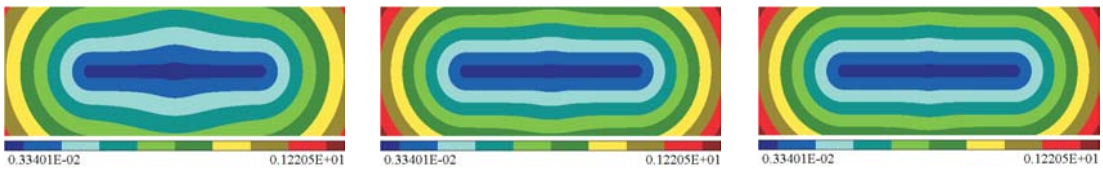

(a) (b) (c)

Fig. 6. (a), (b) and (c) were constructed by h_1 and h_2, distance functions of two line segments with R-equivalence operation of order 2, 7 and 12 respectively.

2.4 Experiments and Discussion

We performed extensive experiments with the proposed approach for constructing approximate distance fields for various planar curves. All curves were first polygonized using tools available in a commercial solid modeling system (Parasolid). Subsequently, normalized functions were constructed for each line segment in the polygonized curve, and then joined into a single field for each test curve using the operations described above. The resulting field was then sampled on 99×99 regular grid and bilinearly interpolated to produce Figures 7 and 2.

Figure 7 shows distance fields constructed from a 4th order B-spline curve in the shape of the letter 'S'. This B-spline curve was polygonized three times with variable precision (maximum deviation

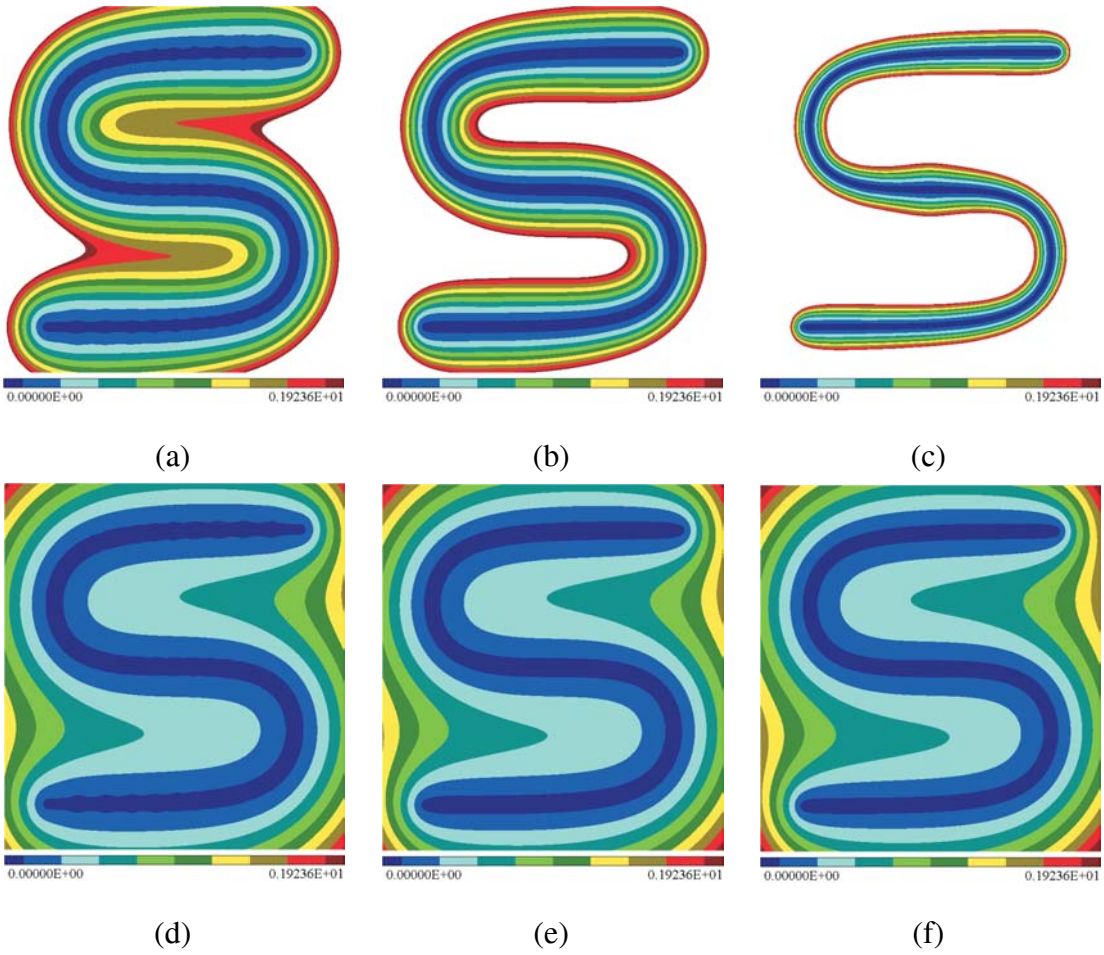

Fig. 7. Isolines of six fields constructed from an 'S' shaped B-spline curve of order 4. Functions in figures (a), (b) and (c) are constructed with R-equivalence of order 2, with an error of polygonization 0.01, 0.001 and 0.00001 respectively. R-conjunction of order 2 is used to construct functions in figure (d), (e) and (f) with an error of polygonization 0.01, 0.001 and 0.00001 respectively.

from the original curve) ϵ: setting ϵ to 0.01, 0.001 and 0.00001 results in 56, 157 and 1499 linear segments respectively. A distance field of a the line segment of the polygonal approximation was constructed by performing the trimming operation with a circular disk and the infinite line as shown in Figure 3. An approximate distance field for each polygonized curve was constructed using second order R-equivalence (top row) and R-conjunction (bottom row). Because the approximation of the distance field is $O(\epsilon)$, more precise polygonization (with smaller ϵ) should produce more accurate distance fields. The increased number of line segments is accompanied by a greater number of joining points, where normalization is lost. However, for a smooth curve as in Figure 7, a more precise polygonization also implies larger angle α between adjacent line segments, bringing the minimum values of gradients closer to 1 in the neighborhood of the joining points. The latter improvement appears to compensate for the increased number of singular points, as can be seen by comparing examples (a), (b), (c) and (d), (e), (f) respectively in Figure 7. In all cases, the constructed field is visibly very close to the curve's distance field in the neighborhood of the curve.

The fields in the bottom row (constructed with R-conjunction) grow visibly slower than those in the top row (constructed with R-equivalence). Near the boundary, the different rates of growth can be attributed to the fact that R-conjunction maintains normalization one order lower than the corresponding R-equivalence. Thus, the fields in the bottom row are normalized to the first order, but the fields in the top row to the second order; producing a much better approximation of the distance function in the vicinity of the curve. In the case of R-conjunction, increasing the precision (and number of segments) of approximation has little effect on the overall quality of the field, but in the case of R-equivalence it is accompanied by increase in the gradient values away from the curve. In Figure 7(c), the change is so rapid that the transitions between the adjacent isolines are difficult to see. We also observe that when the number of segments is sufficiently large, the fields constructed with R-equivalence may exhibit undesirable global effects. Notice the widening of the distance field near the flatter sections of the curve with the increase of segments in the approximation (compare Figures 7(a), (b), and (c)). While visually similar, this widening is in fact not related the local bulging as characterized above, but is caused by global properties of R-functions and trimming regions that are not investigated in this paper.

Recall that the minimum value of gradient in the neighborhood of a joining point always occurs in the convex sector formed by the adjacent line segments. This effect is apparent in all the fields in Figure 7. This is why the isolines of the constructed fields are farther apart on the convex side of the turns in 'S' than on the concave side. This effect is even more prominent for the fields plotted in Figure 2(b), (c), (d), (e) and (f). The fields shown were constructed from a 'W' shaped B-spline curve of order 4 that was polygonized with a maximum error of 0.001 and were normalized to the order 2, 3, 5, 7, and 12 respectively. The increased order of normalization visibly reduces bulging but does not eliminate it, as discussed above. In this example, the distance field of each line segment in the polygonal approximation was obtained by trimming an infinite line by two orthogonal lines passing through the two end points of the line segment. Different choices of trim regions may affect global behavior of the fields but not its normalization properties near the joining points.

3 Three dimensional fields

The proposed approach extends naturally to subsets of d-dimensional space that can be represented (either exactly or approximately) by a union of quasi-disjoint[4] trimmed patches. The patches themselves could be of any dimension, and their union need not be homogeneous. A normalized distance field for a union of patches can always be approximated by joining together the fields constructed for individual trimmed patches. Similarly to the case of planar curves, the properties of the resulting fields will be determined by methods for trimming and joining of constituent fields. Before attempting construction of fields for dimensionally heterogeneous objects, we consider two common types of objects, namely space curves and triangulable surfaces.

[4] Patches are quasi-disjoint when they either do not intersect or intersect on their boundaries only.

3.1 Space curves

The procedure in the last section generalizes to E^3 in a straightforward fashion. Each space curve is approximated by a finite union of linear segments. A normalized function $h(x, y, z)$ for a linear segment in E^3 is constructed using expressions (4) or (5), with normalized functions $f(x, y, z)$ representing a line in E^3 and $t(x, y, z)$ representing a trim volume (for example, a sphere). The normalized function for a line in E^3 can be defined as $f = \sqrt{s^2 + q^2}$, where s and q are normal functions for any two orthogonal planes intersecting along the line. If the boundary of the trim volume is orthogonal to the line at the intersection points, as is the case with the sphere, the resulting function $h(x, y, z)$ is normalized in the generalized sense on all points of the line segment, including its end points.

Joining operations (either R-equivalence or R-conjunction) can be used without modification, and essentially the same error analysis applies. The constructed field is not differentiable at the line segments themselves, but is normalized almost everywhere in the generalized sense. As before, normalization fails in the neighborhoods of joining points, where the magnitude of the gradient of the field varies between 0 and 1. The minimum value of the gradient occurs along the bisector of the angle, α, between adjacent line segments, measured in the plane formed by the two line segments (recall Figure 4). The main difference is that in E^3 this bisector is a plane that corresponds to infinitely many directions in E^3.

Figure 8 shows constructed approximate distance fields on section planes for two space curves. The field for the B-spline curve of degree 3 in Figure 8(a) is constructed from the distance fields of 56 line segments, obtained by the polygonization of the curve, and joining them with R-equivalence of order 2. The distance field of the other (Figure 8(b)) degree 3 B-spline curve is constructed from distance fields of 90 line segments by R-equivalence of order 2. Loss of normalization at the joining points does not appear to distort fields away from the curves.

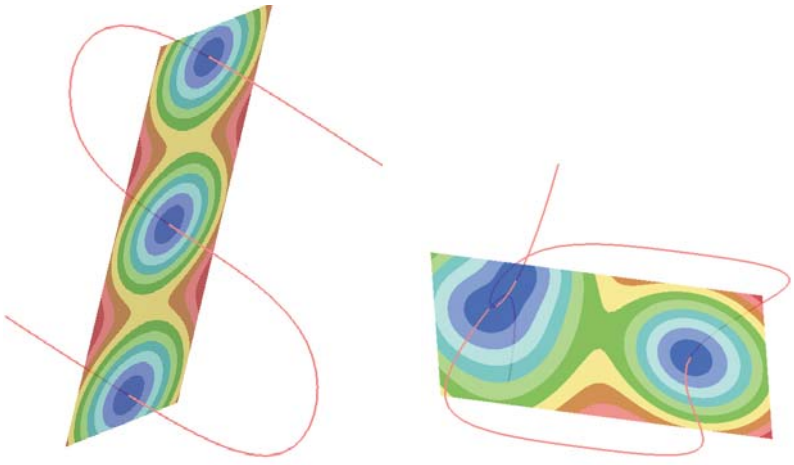

(a) (b)

Fig. 8. Space curves and the constructed distance fields on section planes

3.2 *Surface in E^3*

The proposed field construction method applies to all surfaces that may be decomposed into quasi-disjoint trimmed patches, where each patch is the intersection of some trim volume and an unbounded carrier surface. The decomposition may be exact or approximate. Here we focus on the simplest case, where a surface is represented by a linear triangulation [37,38]. The construction process involves the same two tasks: representation of fields for individual triangles and joining them into a single field. Each task leads to new challenges that are considered in detail below.

3.2.1 *Field for a triangle*

An obvious approach to constructing a field for a triangle relies on representing the triangle as the intersection of its carrier plane $f(x, y, z) = 0$ with the three linear halfspaces $p_i \geq 0$, $i = 1, 2, 3$. Each halfspace is associated with a plane P_i that is orthogonal to the carrier plane and passes through an edge of the triangle (see Figure 9(a)). This approach naturally suggests that the trim volume for the triangle is the triangular unbounded prism formed by intersection of the three trim halfspaces $p_i \geq 0$. A function for such a prism is easily constructed using R-conjunction: $t = p_1 \wedge p_2 \wedge p_3$ [35,29]. As required, function t is positive on all the points of interior of the triangle, zero on its boundary, and negative on all other points of the plane $f = 0$. Substituting this t and f into (4) or (5) yields the desired three-dimensional field $h(x, y, z)$ for the triangle. Unfortunately, the above function t is not differentiable along the edges of the prism that are

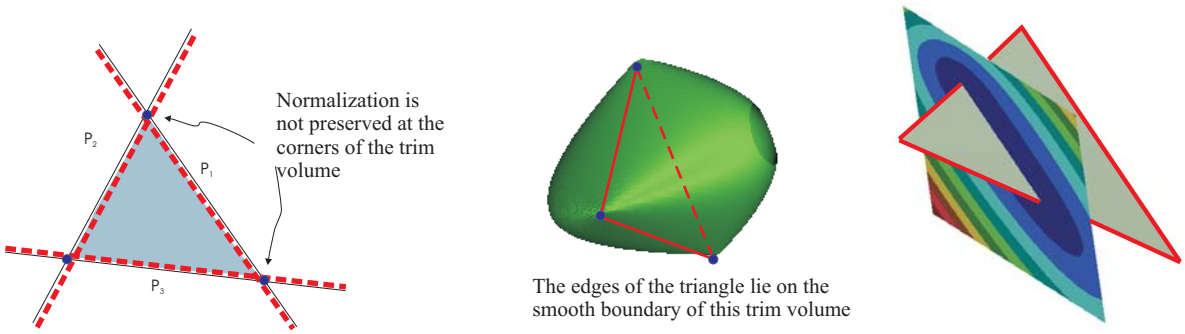

Fig. 9. (a) Trim volume for a triangle is constructed using intersection of the three planes perpendicular to the carrier plane containing the triangle. (b) shows the constructed trim volume. (c) Distance field of a triangle is displayed on a section plane

defined by intersections of planes P_1, P_2, P_3 and which extend throughout the space. This lack of smoothness will be inherited by the constructed field h. If many such fields are joined together for a triangulated surface, the combined field will not be smooth along the numerous lines passing through the vertices in the triangulation of the surface.

Geometrically, the problem arises because the boundary of the trim volume (the prism) has sharp edges extending throughout E^3. Fortunately, the trim volume is not unique, and it is possible to

construct another trim volume with a smoother boundary intersecting the given plane on the edges of the triangle. Such a volume is shown in Figure 9(b), and its construction relies on the notion of *conditional* R-functions [31] as follows. Every R-function can be modified to include additional functional terms, and the resulting function works as R-function *only* when these terms take on certain values. For example, we can replace the usual R-conjunction $p_1 \wedge p_2$ with a new function

$$p_1 \underset{f}{\wedge} p_2 \equiv p_1 + p_2 - \sqrt{p_1^2 + p_2^2 + af^k} \tag{15}$$

which reduces to the usual R-conjunction operation only when $f = 0$. The positive constants a and k may be used to control the shape of the zero set of this function. When $f \neq 0$, corresponding to the points of E^3 not lying on the triangle plane, this function is analytic (and therefore in C^∞). Repeating the construction with all three planes, we obtain function

$$t = p_1 \underset{f}{\wedge} p_2 \underset{f}{\wedge} p_3 \tag{16}$$

whose zero set is the boundary of the trim volume shown in Figure 9(b) for constant values $a = 0.2$ and $k = 2$. It is easy to check that function t is not differentiable only at the vertices of the triangle. In fact, t is normalized everywhere except the vertices where the magnitude of its gradient varies but remains positive and bounded depending on the direction. The detailed analysis is similar to the one in section 2.3 (see [29] for detailed analysis of R-functions).

Combining functions f and t according to equation (4) or (5) yields an approximate distance field h for a given triangle, which is smooth everywhere except the boundary of the triangle. Figure 9(c) shows a triangle and the constructed distance field on a section plane. If the carrier plane $f = 0$ and the three construction planes p_1, p_2, p_3 are represented by their normal functions, then function h is normalized on all interior points of the triangle (in the direction normal to the triangle); h is also normalized in the generalized sense on the edges of the triangle.

However, normalization of h fails in the neighborhoods of the vertices of the triangle where function t is not normalized. The plot in Figure 10(b) is produced by the Mathematica system [39] and shows how the magnitude of the gradient vector ∇h varies in the neighborhood of a sample vertex: it clearly depends on the direction of approach but remains bounded in a relatively tight range.

3.2.2 Joining Operation

Approximate distance fields $h_1, h_2, \ldots, h_n$ for n quasi-disjoint surface patches, such as triangles in a triangulation of a surface, can be combined into a single field $u = F(h_1, \ldots, h_n)$ using the joining operations introduced in section 2.2. As expected, further deterioration in the normalization properties of F occurs at the points where the boundaries of adjacent patches or triangles overlap. Gradient behavior is substantially different in the neighborhoods of edges and vertices, and should be considered separately. By definition, directions normal to the edge of a triangle at a given point lie in the plane perpendicular to the edge at that point(see Figure 11). Therefore, the case of two triangles joined along a common edge in E^3 is a straightforward generalization of the case of two line segments joined at a common point in E^2, as described in section 2.3. Because the individual

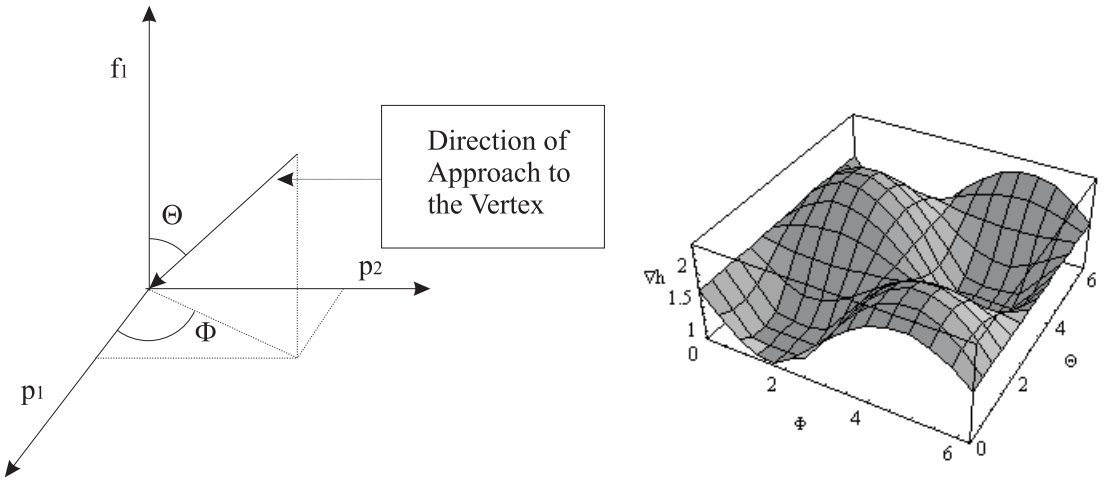

(a) (b)

Fig. 10. Figure (a) shows the coordinate system defined by the functions, whose zero sets intersect to define the vertex of the triangle. Figure (b) shows the absolute value of gradient in the neighborhood of the vertex of the triangle.

triangle fields h_1 and h_2 are normalized in the neighborhood of edges, the magnitude of gradient ∇u of the combined field remains bounded between 0 and 1, and its minimum value occurs along the bisector of the dihedral angle.

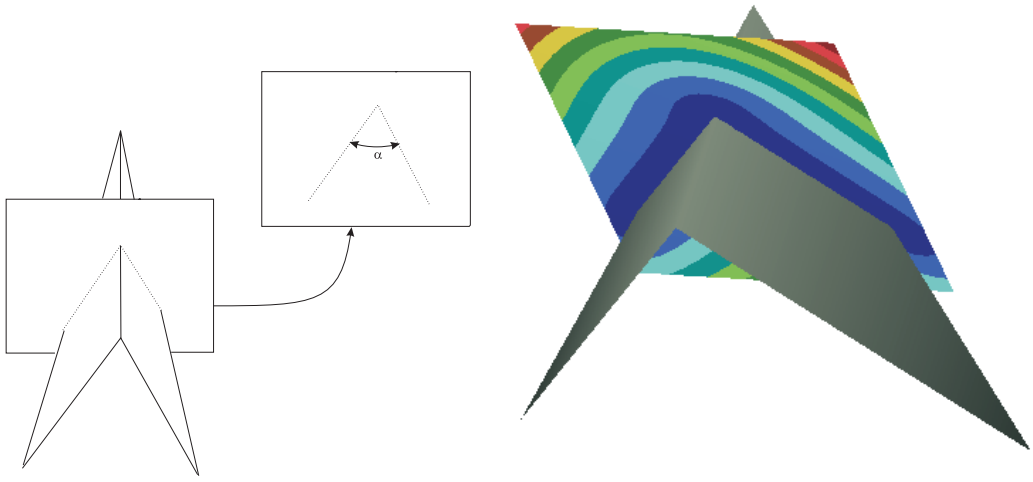

(a) (b)

Fig. 11. Properties of the field for two triangles sharing a common edge are determined by the planar sections orthogonal to the edge (a). (b) shows the distance field on a section plane for two triangles joined with R-equivalence of order 2.

Two additional complications arise in a neighborhood of a shared vertex. Firstly, the individual fields h_1 and h_2 may not be normalized, and secondly, any number of triangles may be joined together at a single vertex. Consider what happens to the gradient of the combined field $u =$

$F(h_1, h_2)$ in the neighborhood of a vertex, where two triangles are joined. Expanding and rewriting Equation (10) in terms of ∇h_1 and ∇h_2, yields

$$|\nabla u|^2 = \left(\frac{\partial F}{\partial h_1}\right)^2 (|\nabla h_1|)^2 + \left(\frac{\partial F}{\partial h_2}\right)^2 (|\nabla h_2|)^2 + 2\frac{\partial F}{\partial h_1}\frac{\partial F}{\partial h_2}(\nabla h_1 \cdot \nabla h_2) \tag{17}$$

$$\leq \left(|\nabla h_1|\frac{\partial F}{\partial h_1} + \frac{\partial F}{\partial h_2}|\nabla h_2|\right)^2 \tag{18}$$

because the product $\nabla h_1 \cdot \nabla h_2 \leq |\nabla h_1||\nabla h_2|$ remains bounded as it varies with direction of approach to the vertex. Recall that both R-equivalence and R-conjunction have positive partial derivatives $\frac{\partial F}{\partial h_1}$ and $\frac{\partial F}{\partial h_2}$ and their sum $(\frac{\partial F}{\partial h_1} + \frac{\partial F}{\partial h_2}) \leq 1$. In the context of the inequality (18) this implies that

$$|\nabla u| \leq \max(|\nabla h_1|, |\nabla h_2|),$$

and therefore, the joining operation does not increase the magnitude of the gradient ∇u in any direction. From Equation (17) it follows that $|\nabla u|$ will necessarily diminish in any direction where the angle between ∇h_1 and ∇h_2 is strictly between 0 and π. As the angle approaches π, $|\nabla u|$ approaches 0 near the joining points but never reaches it. A more precise analysis is difficult because h_1 and h_2 are not normalized in the neighborhood of the vertex.

The effect of joining n triangles at a single vertex should now be clear. If $h_1, h_2, \ldots, h_n$ are approximate fields for each of the triangles that are combined via either R-equivalence or R-conjunction into a single field u, then $|\nabla u| \leq \max(|\nabla h_1|, |\nabla h_2|, \ldots, |\nabla h_2|)$ in the neighborhood of the joining point, but every triangle contributes to further deterioration of the field by increasing a number of directions where $|\nabla u|$ is substantially less than 1.

Figure 12(a) shows a B-spline surface that was triangulated with maximum error of 0.5 and 0.005, and these triangulations were used to construct approximate distance fields. The planar sections of the two distance fields are shown in Figures 12(b) and (c) respectively. Both fields were constructed using R-equivalence as a joining operation, and both were sampled on a regular 99×99 grid for visualization purposes. In all cases, the effects of singularities at the joining points appear to be confined to the neighborhoods of such points and are not noticeable away from the surface.

4 Conclusions

4.1 Relation to other approaches

Broadly, all techniques for constructing smooth approximations of distance fields may be divided into several categories: constructive, interpolation, level sets, and potential function methods. The method described in this paper falls into the category of constructive approximations. For comparison, let us briefly consider other approaches.

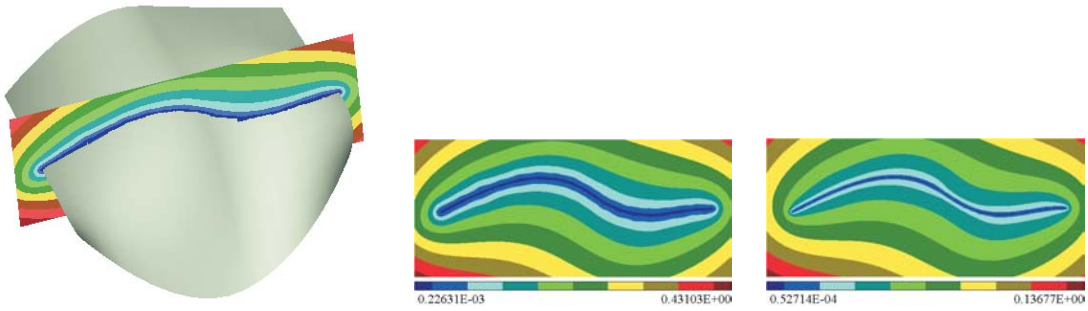

(a) (b) (c)

Fig. 12. A (3,4) order B-spline surface (a) along with the plane on which its implicit representation is studied; (b) and (c) are plots on the plane shown in (a). The approximate distance fields were constructed with R-equivalence of order 2 and with the polygonal approximation, with an error of polygonization .05 and .005 respectively.

Interpolation methods have been used by many to construct implicit representations for curves and surfaces [40–43]. To construct an approximate distance field for a set S, one could sample the distance to S with desired resolution and interpolate the results using B-splines, radial basis, or other convenient basis functions. In addition to the usual numerical issues arising with any such approach, the constructed approximation will have at least two additional limitations. The accuracy of the approximate field will depend on both resolution of sampling and choice of the basis; this in turn may limit its usefulness when the field must be defined globally, yet capture small geometric details. Secondly, assuring normalization properties (to some order) is likely to be problematic, because in the neighborhood of S, the gradient of the interpolated functions may have flat spots (where the gradient vanishes).

Readers familiar with level set methods [10,44] may have noticed the similarity of level sets to approximate distance fields [45]. Both are defined by smooth functions whose level sets (iso-curves, iso-surfaces, etc.) propagate from the given set of points. In the case of level sets, the speed of propagation is usually selected as a function $V(\kappa) = 1 - e\kappa$, where κ is the curvature, and e is an application dependent (typically small) constant. The approximate field is defined implicitly and requires repeated numerical evaluation in order to determine level sets at a distance away from the starting set of points. Recall that with our approach the normalization of the field is violated in the neighborhood of joining points, where the unit gradient decreases in proportion to the angle between adjacent patches following the relation (11). This is analogous to prescribing the speed of the level sets as a function of curvature, but the resulting field is defined globally and explicitly.

Another promising method for approximating distance fields relies on the observation that the reciprocal of a distance field to a set S may be approximated by a potential function

$$f(\mathbf{x}) = \int_S \frac{1}{r(\mathbf{x})^n} dS, \tag{19}$$

where $r(\mathbf{x})$ measures the distance from point $\mathbf{x}$ to dS [46]. As n increases, the influence of points of S farther away decreases, giving a measure of the distance as $n \to \infty$. In addition to $\frac{1}{r(\mathbf{x})^n}$,

a number of other kernels have been proposed by advocates of convolution methods [30,47], including Gaussian, Cauchy, polynomials, and many others. Potential and convolution fields share many attractive properties. The integral formulation may be convenient for parametric curves and surfaces and may lead to closed form representations for some simple sets such as line segments and circular arcs[47]. As global sums over all points of a set, convolution fields avoid bulging, making them a popular choice in computer graphics. However, differential properties of the constructed functions $f(\mathbf{x})$ depend on the selected kernels. Most popular choices of kernels lead to fields that cannot be normalized. For example, fields constructed with polynomial and exponential kernels are flat on the boundary (i.e., the derivatives normal to S vanish). Differential properties of singular kernels of the form $\frac{1}{r(\mathbf{x})^n}$ depend on n, but they are notoriously difficult to evaluate due to numerical instabilities[48]. Nevertheless, potential fields with singular kernels poses sufficiently attractive properties to warrant further investigation. In particular, notice that the R-equivalence operation (6) has essentially the same form as the potential function (19), with each h_i measuring a distance to a set of points as opposed to a single point $\mathbf{x}$.

4.2 Summary and Extensions

The virtues of the proposed approach for constructing approximate distance fields with non-vanishing gradients include simplicity and generality. It can be applied to geometric models of virtually any shape or topology. In all cases, the constructed approximate distance field is as precise as the geometry of each segment and is normalized everywhere except the joining points. Figure 13 shows distance fields of a 2-D set of heterogeneous dimension in (a), a trimmed B-spline surface in (b), and a simple polyhedral solid in (c). In each case, the distance field was obtained by joining individual fields of trimmed curves, surfaces, or points that were constructed using techniques described in sections 2 and 3. We have not studied global properties of the constructed fields, but it should

(a) (b) (c)

Fig. 13. (a) Approximate distance field of a square region, a line segment and a point (dimensions 2,1 and 0 respectively); (b) a section of a field for a trimmed surface generated by a lofting operation in a commercial geometric modeler; (c) a section of a distance field for a simple polyhedral solid.

be clear that the fields are defined and are sufficiently smooth everywhere. Because the fields are represented explicitly in a closed form that does not require search or iteration, they are easy to differentiate, sample, and integrate. In particular, automatic differentiation techniques [49] allow

computation of derivatives of any order exactly. These properties of the constructed fields make them highly suitable for material modeling[5] and meshfree analysis [6,23].

The main drawback of the proposed method is the potentially large size of the constructed representation when a curve or a surface is approximated by a large number of small segments. In principle, the same constructive method can be applied to any and all piecewise implicit representations of curves and surfaces. In this case, each trimmed entity is represented as the intersection of an unbounded carrier (curve or surface) with a trim volume[50]. If the unbounded carrier and the trim volume are represented implicitly by normalized functions f and t respectively, then an approximate distance field is constructed precisely in the same manner as described in section 2.1. This observation could be used to substantially reduce the number of required segments, and in particular the same approach is applicable to any union of quasi-disjoint smooth patches that may be of higher order and arbitrary shape. By definition, such constructive representations exist theoretically for all semi-analytic sets. The problem of obtaining a constructive representation for an implicitly defined trimmed curve or surface is an instance of a more general problem known as boundary to CSG conversion[51,52]. Moreover, implicit representations are not available for most parametric curves and surfaces that are now in common use in solid modeling systems. In principle, any parametric representation may be converted into an implicit one using any one of several known implicitization procedures, but practical solutions are currently limited. Implicitization techniques include algebraic resultant-based elimination [53], Gröbner bases methods [54], moving curves and surfaces [55], and various approximate implicitization schemes [56–58]).

Our experience shows that the constructed fields are adequate in most practical situation, despite the loss of normalization near the joining points. Nevertheless it is reasonable to ask whether normalization at *all* points is feasible. The affirmative answer follows immediately from the observation that any field with non-vanishing gradient may be scaled as described in Appendix A. However, practical application of scaling may be problematic because it increases both computational cost and the required order of differentiability of the field.

Another possible approach is to modify the joining operations directly to take into account geometry of the neighborhood where the patches are joined. Recall that in the neighborhood of a joining point, the normal is defined (in the generalized sense) only in the concave sector (Figure 4(b)). Thus there is no reason to expect that $|\nabla u| = 1$ in the convex sector; in fact, this would violate normalization of u on regular points in the neighborhood of the joining point. In the concave sector, u is normalized in all directions except the hatched sector corresponding to the set of points that are equidistant from both line segments and the joining point. If the field u were also normalized in this sector, it would have been equal to a normalized field q measuring the distance to the joining point. Instead, if u is constructed using R-equivalence (6), it is easy to check that $u = 1/\sqrt[p]{\frac{2}{q^p}}$ in the neighborhood of the joining point, because $h_1 = h_2 = q$. Recall that R-equivalence (6) is defined in terms of the reciprocal of the p-norm of the vector $(\frac{1}{h_1}, \frac{1}{h_2})$ but this apparently overestimates the expression under the pth root by $(1/q)^p$. Modifying R-equivalence to

$$F(h_1, h_2, q) = \frac{1}{\sqrt[p]{\frac{1}{h_1^p} + \frac{1}{h_2^p} - \frac{1}{q^p}}} = \frac{h_1 h_2 q}{\sqrt[p]{(h_1 q)^p + (h_2 q)^p - (h_1 h_2)^p}} \tag{20}$$

does not affect normalization of $u = F(h_1, h_2, q)$ on regular point and forces $|\nabla u| = 1$ in the hatched sector.

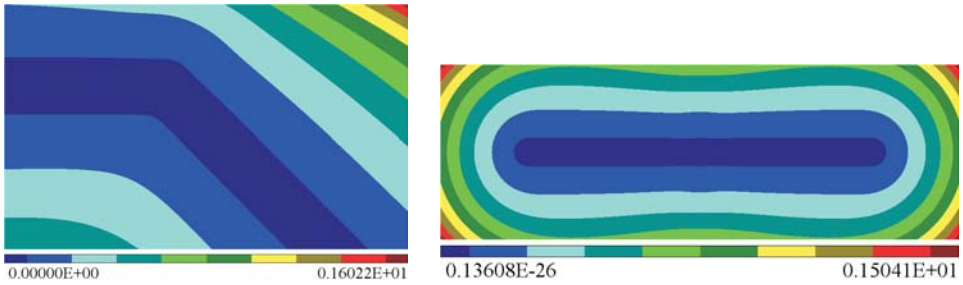

(a) (b)

Fig. 14. (a) and (b) are corrected fields for union of two line segments in Figure 1(c) and Figure 6(a) respectively.

Figure 14(a) shows the resulting field for the union of the two line segments in Figure 1 with q chosen as the exact distance to the joining point. Compare the corrected field in Figure 14(b) for two collinear segments to those constructed with the regular R-equivalence in Figure 6(a). Similar techniques were used experimentally in [36] for modeling of solidification in metal castings.

These examples suggest that it may be possible to construct fields normalized at all points for arbitrary decompositions of curves and surfaces. For higher-order patches, the magnitude of the gradient in neighborhoods of joining points varies depending on the local geometry of the tangent spaces, which could be used to design improved joining operations. Normalization at all points of the boundary is not sufficient to assure that a constructed approximation behaves as a distance field globally. The global properties of the constructed fields, including smoothness, remain to be explored.

Appendix

A Recursive Normalization of Functions to m-th Order

Any function, f, with non-vanishing gradient near its zero set can be normalized to the m-th order using the recursive formulation, introduced in [31]. The transformation process involves two steps. First, a function f is normalized to the first order as:

$$f_1 = \frac{f}{\sqrt{f^2 + (\nabla f)^2}} \tag{A.1}$$

For functions already normalized to the first order, this transformation is not required.

In the second step, given a function f_m normalized to the order m, $m \geq 1$, a new function f_{m+1} is

constructed by employing the recursive formulation:

$$f_2 = f_1 - \frac{1}{2!} f_1^2 \frac{\partial^2 f_1}{\partial \nu^2} \tag{A.2}$$

$$f_3 = f_2 - \frac{1}{3!} f_1^3 \frac{\partial^3 f_2}{\partial \nu^3} \tag{A.3}$$

$$\dots$$

$$f_m = f_{m-1} - \frac{1}{m!} f_1^m \frac{\partial^m f_{m-1}}{\partial \nu^m} \tag{A.4}$$

Acknowledgments

This work was supported in part by the National Science Foundation grants DMI-9900171, DMI-0115133, and CCR-0112758, General Motors Corporation, EDS PLM Solutions and NIST grant 60NANB2D0126. Vadim Shapiro gratefully acknowledges the support from the Department of Computer Science and Automation of the "Roma Tre" University, Italy that allowed him to continue research on this and other problems during his sabbatical visit.

References

[1] A. Pasko, M. S. (eds), Proceedings of International Conference on Shape Modeling and Applications, IEEE Computer Society, Genova, Italy, 2001.

[2] H. Liu, W. Cho, T. R. Jackson, N. M. Patrikalakis, E. M. Sachs, Algorithms for design and interrogation of functionally gradient material objects, in: Proceedings of 2000 ASME DETC/CIE, 26-th ASME Design Automation Conference,Baltimore, Maryland, 2000, p. 141.

[3] S.-M. Park, R. H. Crawford, J. J. Beaman, Volumetric multi-texturing for functionally gradient material representation, in: Proceedings sixth ACM symposium on Solid modeling and applications, ACM Press, 2001, pp. 216–224.

[4] Y. K. Siu, S. T. Tan, Source-based heterogeneous solid modeling, Computer-Aided Design 34 (2002) 41–55.

[5] A. Biswas, V. Shapiro, I. Tsukanov, Heterogeneous material modeling with distance fields, Tech. Rep. SAL2002-4, SAL, Mechanical Engineering Department, University of Wisconsin, Madison, WI-53706 (2002).

[6] V. L. Rvachev, T. I. Sheiko, R-functions in boundary value in mechanics, Applied Mechanics Reviews 48 (4) (1995) 151–188.

[7] E. Hartmann, Numerical implicitization for intersection and g^n continuous blending of surfaces, Computer Aided Geometric Design 15 (1998) 377–397.

[8] K. Museth, D. E. Breen, R. T. Whitaker, A. H. Barr, Level set surface editing operators, in: Proceedings of the 29th annual conference on Computer graphics and interactive techniques, ACM Press, 2002, pp. 330–338.

[9] E. Hartmann, Numerical parameterization of curves and surfaces, Computer Aided Geometric Design 17 (2000) 251–266.

[10] J. Sethian, Level Set Methods and Fast Marching Methods, 2nd Edition, Cambridge University Press, Cambridge, UK, 1999.

[11] G. T. Herman, J. Zheng, C. A. Boucholtz, Shape-based interpolation, IEEE Computer Graphics and Applications 12 (1992) 69–79.

[12] S. F. Frisken, R. N. Perry, A. P. Rockwood, T. R. Jones, Adaptively sampled distance fields: a general representation of shape for computer graphics, in: Proceedings of the 27th annual conference on Computer graphics and interactive techniques, ACM Press/Addison-Wesley Publishing Co., 2000, pp. 249–254.

[13] R. S. Avila, L. M. Sobierajski, A haptic interaction method for volume visualization, in: Proceedings of the conference on Visualization '96, IEEE Computer Society Press, 1996, pp. 197–204.

[14] E. Hartmann, The normalform of space curve and its application to surface design, The visual computer 17 (7) (2001) 445–456.

[15] R. Blanding, C. Brooking, M. Ganter, D. Storti, A skeletal-based solid editor, in: Proceedings of the fifth symposium on Solid modeling and applications, ACM Press, 1999, pp. 141–150.

[16] S. F. F. Gibson, Using distance maps for accurate surface representation in sampled volumes, in: Proceedings of the 1998 IEEE Symposium on Volume visualization, ACM Press, 1998, pp. 23–30.

[17] D. Cohen-or, D. Levin, A. Solomovici, Three-dimensional distance field metamorphosis, ACM Transaction on Graphics 17 (2) (1998) 116–141.

[18] D. E. Breen, R. T. Whitaker, A level-set approach for the metamorphosis of solid models, IEEE Transactions on Visualization and Computer Graphics 7 (2) (2001) 173–192.

[19] J.-C. Latombe, Robot Motion Planning, Kluwer Academic Publishers, Boston/Dordrecht/London, 1991.

[20] J. Lengyel, M. Reichert, B. R. Donald, D. P. Greenberg, Real-time robot motion planning using rasterizing computer graphics hardware, in: Proceedings of the 17th annual conference on Computer graphics and interactive techniques, ACM Press, 1990, pp. 327–335.

[21] M. Garber, M. C. Lin, Constraint-based motion planning using voronoi diagrams, in: Proceeding of the Fifth International Workshop on Algorithmic Foundations of Robotics, WAFR, 2002.

[22] M. E. Mortensen, Geometric Modeling., John Wiley and Sons, New York, 1985.

[23] I. Tsukanov, V. Shapiro, The architecture of SAGE – a meshfree system based on RFM, Engineering with Computers 18 (4) (2002) 295–311.

[24] V. Rvachev, T. Sheiko, V. Shapiro, I. Tsukanov, Transfinite interpolation over implicitly defined sets, Computer-Aided Geometric Design 18 (4) (2001) 195–220.

[25] B. A. Payne, A. W. Toga, Distance field manipulation of surface models, IEEE Computer Graphics and Applications 12 (1992) 65–71.

[26] J. Bloomenthal, Introduction to Implicit Surfaces, Morgan Kaufmann Publishers, 1997.

[27] A. Ricci, A constructive geometry for computer graphics, The Computer Journal 16 (2) (1973) 157–160.

[28] A. P. Rockwood, J. Owen, Blending surfaces in solid modeling, in: G. E. Farin (Ed.), In Geometric Modeling: Algorithms and New Tremds, SIAM, Philadelphia, Pa, 1987.

[29] V. Shapiro, I. Tsukanov, Implicit functions with guaranteed differential properties, in: Fifth Symposium on Solid Modeling and Applications,Ann Arbor,Michigan, 1999, pp. 258–269.

[30] J. Bloomenthal, Bulge elimination in implicit surface blends, in: Implicit Surfaces'95, Grenoble, France, 1995, pp. 7–20.

[31] V. L. Rvachev, Theory of R-functions and Some Applications, Naukova Dumka, 1982, in Russian.

[32] B. Wyvill, E. Galin, A. Guy, Extending The CSG Tree. Warping, Blending and Boolean Operations in an Implicit Surface Modeling System, Computer Graphics Forum 18 (2) (1999) 149–158.

[33] P. S. Heckbert, Graphics Gem, Vol. 4, AP Professional, 1994.

[34] W. DAHMEN, Subdivision algorithms converge quadrically, Journal of Computational and Applied Mathematics 16 (1986) 145–158.

[35] V. Shapiro, Theory of R-functions and applications: A primer, Tech. rep., Cornell University (November 1988).

[36] V. L. Rvachev, T. I. Sheiko, V. Shapiro, J. J. Uicker, Implicit function modeling of solidification in metal casting, ASME Journal of Mechanical Design 119 (1997) 466–473.

[37] L. A. Piegl, W. Tiller, Geometry-based triangulation of trimmed nurbs surfaces, Computer-Aided Design 30 (1) (1998) 11–18.

[38] G. Elber, Error bounded piecewise linear approximation of freeform surfaces, Computer-Aided Design 28 (1) (1996) 51–57.

[39] S. Wolfram, The Mathematica book, 4th Edition, Wolfram Media, Champaign, IL and Cambridge University Press, Cambridge, UK, 1997.

[40] A. Raviv, G. Elber, Three dimensional freeform sculpting via zero sets of scalar trivariate functions, in: Proceedings of the fifth ACM symposium on Solid modeling and applications, ACM Press, 1999, pp. 246–257.

[41] P. B. J. Esteve, A. Vinacua, Multiresolution for algebraic curves and surfaces using wavelets, Computer Graphics Forum 20 (1) (2001) 47–58.

[42] V. V. Savchenko, A. A. Pasko, O. G. Okunev, T. L. Kunii, Function representation of solids reconstructed from scattered surface points and contours, Computer Graphics Forum 14 (4) (1995) 181–188.

[43] G. Turk, J. F. O'Brien, Shape transformation using variational implicit functions, in: Proceedings of the 26th annual conference on Computer graphics and interactive techniques, ACM Press/Addison-Wesley Publishing Co., 1999, pp. 335–342.

[44] S. Osher, R. Fedkiw, Level Set Methods and Dynamic Implicit Surfaces, Springer, Berlin, 2002.

[45] D. Breen, S. Mauch, R. Whitaker, 3D scan conversion of CSG models into distance, closest-point and colour volumes, in: M. Chen, A. Kaufman, R. Yagel (Eds.), Volume Graphics, Springer, London, 2000, pp. 135–158.

[46] N. Ahuja, J.-H. Chuang, Shape representation using generalized potential field model, IEEE Transaction Pattern Analysis and Machine Intelligence 19 (2) (1997) 169–176.

[47] A. Sherstyuk, Kernel functions in convolution surfaces: a comparative analysis, The Visual Computer 15 (4) (1999) 171–182.

[48] E. D. Lutz, Numerical methods for hypersingular and near-singular boundary integrals in fracture mechanics, Ph.D. thesis, Department of Computer Science, Cornell University, Ithaca, New York (May 1991).

[49] I. Tsukanov, M. Hall, Data structure and algorithms for fast automatic differentiation, International Journal for Numerical Methods in Engineering 56 (13) (2003) 1949–1972.

[50] J. R. Rossignac, CSG formulations for identifying and for trimming faces of CSG models, in: CSG 96, Information Geometers, 1996, pp. 1–14.

[51] V. Shapiro, D. L. Vossler, Construction and optimization of CSG representations, Computer-Aided Design 23 (1) (1991) 4–20.

[52] V. Shapiro, D. L. Vossler, Separation for boundary to CSG conversion, ACM Transactions on Graphics 12 (1) (1993) 35–55.

[53] T. W. Sederberg, D. C. Anderson, R. N. Goldman, Implicit representation of parametric curves and surfaces, Computer Vision, Graphics, and Image Processing 28 (1) (1984) 72–84.

[54] C. M. Hoffmann, Geometric and Solid Modeling, Morgan Kaufmann Publishers, Inc., 1989.

[55] T. W. Sederberg, F. Chen, Implicitization using moving curves and surfaces, in: Computer Graphics Annual Conference Series, 1995, pp. 301–308.

[56] J. H. Chuang, C. M. Hoffmann, On local implicit approximation and its applications, ACM Transaction on Graphics 8 (4) (1989) 298–324.

[57] Y. de Montaudouin, W. Tiller, H. Vold, Applications of power series in computational geometry, Computer-Aided Design 18 (10) (1986) 93–108.

[58] T. W. Sederberg, J. Zheng, K. Klimaszewski, T. Dokken, Approximate implicitization using monoid curves and surfaces, Graphics Models and Image Processing 61 (4) (1999) 177–198.